International Journal of Thermal Sciences 48 (2009) 1452–1459

Contents lists available at ScienceDirect

International Journal of Thermal Sciences

www.elsevier.com/locate/ijts

# Neural network approach for food temperature prediction during solar drying

P.P. Tripathy, Subodh Kumar *

*Centre for Energy Studies, Indian Institute of Technology, Hauz Khas, New Delhi 110016, India*

ARTICLE INFO

*Article history:*
Received 24 June 2008
Received in revised form 20 October 2008
Accepted 20 November 2008
Available online 20 December 2008

*Keywords:*
Solar drying
Artificial neural network
Heat diffusion model
Laplace transform
Statistical model
Food temperature prediction

ABSTRACT

In the present study, the application of artificial neural network (ANN) for prediction of temperature variation of food product during solar drying is investigated. The important climatic variables namely, solar radiation intensity and ambient air temperature are considered as the input parameters for ANN modeling. Experimental data on potato cylinders and slices obtained with mixed mode solar dryer for 9 typical days of different months of the year were used for training and testing the neural network. A methodology is proposed for development of optimal neural network. Results of analysis reveal that the network with 4 neurons and logsig transfer function and trainrp back propagation algorithm is the most appropriate approach for both potato cylinders and slices based on minimum measures of error. In order to test the worthiness of ANN model for prediction of food temperature variation, the analytical heat diffusion model with appropriate boundary conditions and statistical model are also proposed. Based on error analysis results, the prediction capability of ANN model is found to be the best of all the prediction models investigated, irrespective of food sample geometry.



## 1. Introduction

Moisture removal from food materials by thermal drying is an integral part of food processing. In the past, continuous efforts of the food processing industry for producing dehydrated foods have been directed towards enhancing drying rate, reducing energy consumption and minimizing thermal degradation of food constituents. Increasing mass transfer rates with the help of using higher drying air temperature would result in high energy cost and quality degradation of food product. Processes that facilitate mass transfer of product without adversely affecting quality might be better alternatives for enhancing drying rates and saving energy cost. Decreasing availability of fossil based energy sources with continuously rising energy demands for process heat and consistently increasing prices as well as their adverse environmental impacts have increased the emphasis on the use of most promising renewable energy source such as solar energy, especially for developing countries like India. The application of solar energy in drying of food products has tremendous potential, since it can easily provide the low temperature heating required for drying. It is found that the use of solar dryer system with an efficiency of 40% decreases consumption of conventional energy by 27–80% [1].

Convective solar drying is a simultaneous heat and mass transfer process where heat is transferred by convection from surrounding hot air to the air–food interface and by conduction to the interior of food. Water is transferred by diffusion from inside the food material to air–food interface, and from the interface to the air stream by convection. The knowledge of food temperature variation during solar drying is necessary so as to obtain the information for its safe value that ensures the quality of food product in terms of color, nutrients etc., since the higher sample temperatures often cause food deterioration [2]. The food temperature during solar drying is strongly dependent on various inter-dependent variables such as design parameters of dryer system, climatic conditions and type of food product to be dried. It is observed that for a given food product-dryer system, the climatic parameters namely solar radiation intensity and ambient air temperature significantly influence food temperature and hence drying kinetics.

Mathematical modeling of heat transfer during food processing has been the focus of many studies [3,4]. Models are frequently used as the tools to estimate appropriate heating or cooling times for foods to optimize the quality. In the past, researchers have solved analytically several inter-dependent quasi-steady state energy balance equations of various components of solar dryers for food temperature prediction [5–7]. However, such models are not widely used because of their complexity and long computing time required for their solution. More recently, Rahman and Kumar [8] have applied Laplace transform to solve heat diffusion equation with appropriate boundary conditions for food temperature prediction during drying. It is worth mentioning that with an aim to simplify analysis; these mathematical models consider some basic assumptions while neglecting the effect of several inter-dependent variables, thus result in a decreased prediction capability. In such situation, where the relationship between various variables describing drying problem is complex and ill-defined, the widely

* Corresponding author. Tel.: +91 11 2659 6409; fax: +91 11 2658 1121.
*E-mail address:* subodh@ces.iitd.ernet.in (S. Kumar).

1290-0729/$ – see front matter © 2008 Published by Elsevier Masson SAS.
doi:10.1016/j.ijthermalsci.2008.11.014

**Nomenclature**

| | | |
|---|---|---|
| $a$ | thermal diffusivity of the food product | $m^2/s$ |
| $C_p$ | specific heat capacity of the food product | J/kg °C |
| $h_c$ | convective heat transfer coefficient | $W/m^2$ °C |
| $J_1(\mu_1)$ | first-order Bessel function of the first kind | |
| $J_o(\mu_1)$ | zeroth-order Bessel function of the first kind | |
| $k$ | drying constant | 1/s |
| $k_p$ | thermal conductivity of the food product | W/m °C |
| $L$ | half thickness of slice | m |
| MAE | mean absolute error | |
| $q_s$ | incident solar radiation | $W/m^2$ |
| $R$ | radius of cylinder | m |
| RMSE | root mean square error | |
| $s$ | transform variable | |
| SE | standard error | |
| $T$ | temperature of drying air | °C |
| $t$ | time | s |
| $T_a$ | temperature of ambient air | °C |
| $T_p$ | temperature of food product | °C |
| $W(t)$ | drying rate | $kg/m^2$ s |

*Greek symbols*

| | | |
|---|---|---|
| $\lambda$ | latent heat of vaporization | J/kg |
| $\rho$ | density of potato | $kg/m^3$ |
| $\mu$ | root of the characteristic equation | |

*Subscripts*

| | |
|---|---|
| $o$ | at the beginning of drying |

*Dimensionless terms*

| | |
|---|---|
| $\theta_{wb}$ | characteristic temperature |
| $Bi_h$ | Biot number for heat transfer |
| $Fo$ | Fourier number |
| $k_o$ | lag factor |
| $Pd$ | Predvoditelev number |

used artificial neural network (ANN) can play a decisive role in solving the problem with a reasonable accuracy. Extensive studies on the application of ANN over a wide range of fields were published in the literature for modeling and prediction in energy-engineering systems [9,10]. The systems investigated were: solar steam-generator; solar water heating system; heating, ventilation and air conditioning (HVAC) systems; power generating systems; photovoltaic systems etc. Both of these studies demonstrated the significance and usefulness of ANN in variety of energy related applications. In addition, the literature review indicates that a number of previous studies have used ANN application for predicting the performance of various solar energy systems namely box-type solar cooker [11]; solar water heater [12,13]; solar tunnel dryer [14]; flat plate solar collector [15]. Although extensive studies on the application of ANN to the modeling, performance evaluation etc. of various solar energy systems have been published in the literature, the much needed aspect on transient temperature prediction of food product during solar drying has not received due attention of researchers. Thus, the major objectives of the present study are: to develop and evaluate ANN model of various configurations for temperature prediction of potato cylinders and slices during solar drying based on measures of error deviation from experimental data; to compare the prediction results of developed ANN model with those obtained with analytical heat diffusion and statistical models for testing its worthiness for such application.

## 2. Materials and methods

### 2.1. Experimental arrangement

The potatoes purchased from the local market were cut manually into cylindrical samples of length 0.05 m and diameter 0.01 m and slices of diameter 0.05 m and thickness 0.01 m. A laboratory scale natural convection mixed-mode solar dryer was designed and fabricated to perform the drying experiments on potato samples (Fig. 1). It consisted of an inclined flat-plate solar collector connected in series to a drying chamber in which the food product to be dried is placed on wire mesh tray. The collector-dryer assembly was made of matt black painted 22 gauge (0.64 mm thickness) aluminum sheet used as solar radiation absorber surface with 3 mm thick transparent glass cover on the top to allow solar radiation. Rubber gasket was also used beneath the glass cover for making the system air leak-proof. The fibre glass insulation of thickness 50 mm was provided at the bottom and sides of the assembly to minimize the thermal losses through conduction. The whole assembly was encased in a thick wooden frame with an outer aluminum foil cover to protect it from weather conditions. Two rectangular openings of size 0.305 × 0.05 m at the collector inlet and dryer outlet were made for natural circulation of air by the buoyancy effect due to temperature difference between hot air inside and ambient air outside of the dryer.

### 2.2. Instrumentation and measurements

The temperatures of food samples and drying air (accuracy ±0.1 °C) were measured by calibrated chromel–alumel thermocouples with the help of micro-voltmeter through a selector switch. Several thermocouples were fixed at different locations just beneath the sample surfaces as well as under the wire mesh tray. A schematic diagram of the dryer showing the locations of thermocouples is presented in Fig. 1. During the drying period, the sample weight loss was measured at regular intervals of time, using a precision electronic balance (accuracy ±0.01 g). Moisture content (dry basis) of food product was calculated from weight loss data and dry solid weight of the samples [16].

## 3. Food temperature prediction models

### 3.1. ANN model

The artificial neural network model development generally involves the use of experimental data for training of ANN model, evaluation of various ANN configurations leading to selection of an optimal configuration and its validation with a data set different from those used in training. The major objective of present study is to develop the most appropriate ANN model for prediction of transient temperature ($T_p$) of food in mixed mode solar dryer with easily measurable input variables namely-solar radiation intensity ($q_s$) and ambient air temperature ($T_a$). Thus, in the proposed methodology, the input data involving 94 and 86 experimental data points on each variable $q_s$ and $T_a$ for respective cylinders and slices obtained for several typical days of drying were divided into two sets: training and testing sets. The ANN model was trained using randomly selected 79 and 64 data for cylinders and slices while the remaining 15 and 22 data points were utilized for testing of network performance. The most frequently used feed forward back propagation network structure with input, output and hidden layer was used [17,18]. The number of the neurons in the input layer and output layer are equal to the number

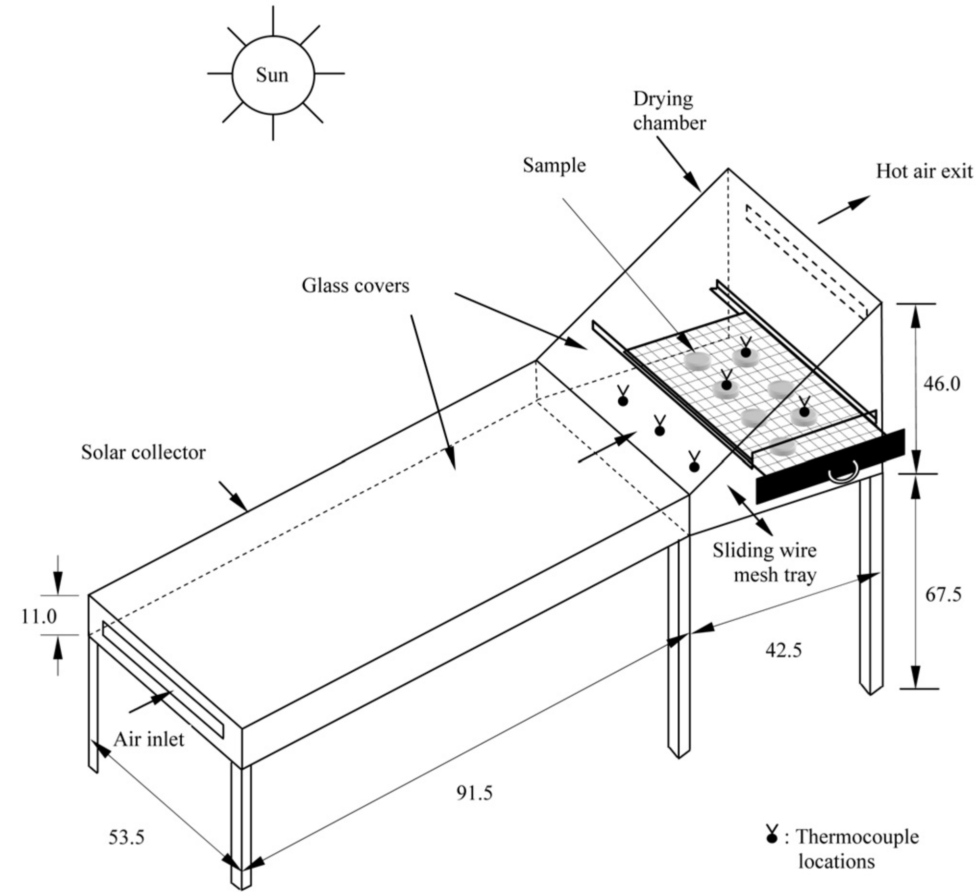


**Fig. 1.** Schematic diagram of the mixed-mode solar dryer. (The dimensions are in cm.)

of input and output parameters respectively. In the present study, the input layer consisted of two neurons corresponding to climatic parameters namely solar radiation intensity and ambient air temperature while the output layer had one neuron representing the transient food product temperature. In this study, one hidden layer was found to be appropriate to develop the model. However, the number of hidden layers and neurons within each hidden layer can be varied based on the complexity of the problem and data set. The ANN model was independently developed for each of potato cylinders and slices. Matlab version 7.0, a popular numerical computation and visualization software, was used for training and testing of neural network.

*3.1.1. Methodology for development of optimal ANN configuration*

In the present work, the most common trial and error approach coupled with iteration technique is employed to develop ANN model. The methodology for performance assessment of network architecture involves obtaining the minimum statistical measures of error between experimental and predicted transient food temperature obtained from prediction model. In this study, statistical measures namely, mean absolute error (MAE), root mean square error (RMSE), standard error (SE) and correlation coefficient ($R^2$) represented by Eqs. (1)–(4) are computed to check the performance of the developed model.

$$\text{Mean absolute error} = \frac{1}{N}\sum_{i=1}^{N}\left|\overline{T}_{p,\exp,i} - \overline{T}_{p,\mathrm{cal},i}\right| \tag{1}$$

$$\text{Root mean square error} = \left[\frac{1}{N}\sum_{i=1}^{N}(\overline{T}_{p,\exp,i} - \overline{T}_{p,\mathrm{cal},i})^2\right]^{1/2} \tag{2}$$

$$\text{Standard error} = \frac{\sqrt{\sum_{i=1}^{N}(T_{p,\exp,i} - T_{p,\mathrm{cal},i})^2}}{N-1} \tag{3}$$

Correlation coefficient ($R^2$)

$$= \sqrt{\frac{\sum_{i=1}^{N}(T_{p,\exp,i} - \overline{T}_{p,\exp,i})^2 - \sum_{i=1}^{N}(T_{p,\exp} - T_{p,\mathrm{cal},i})^2}{\sum_{i=1}^{N}(T_{p,\exp,i} - \overline{T}_{p,\exp,i})^2}} \tag{4}$$

where $\overline{T}_{p,\exp,i}$ and $\overline{T}_{p,\mathrm{cal},i}$ are the average experimental and calculated food sample temperatures for the $i$th observation respectively; $N$ is the number of observations. A well-trained ANN model should produce small MAE, RMSE and SE with large $R^2$ values.

One of the most difficult tasks in ANN model development is to find the optimal network architecture. This network architecture is to be selected out of several network configurations comprising the combination of various model parameters namely, the number of neurons in the hidden layers, different transfer functions and the training algorithms. A list of different transfer functions and training algorithms investigated during training network is summarized in Table 1. Initially, the performance of ANN model is assessed with some specific number of neurons with randomly chosen transfer function and the training algorithms. Subsequently, each of model parameter is varied, keeping the other parameters constant to study the influence of variable parameter on network performance. The iteration process of performance assessment is continued till the most appropriate model that simulates the experiment best based on minimum statistical measures of error is obtained.

In order to obtain the optimum number of neurons in the hidden layer for each of sample geometry, ANN model is trained with varying number of neurons and randomly chosen logsig transfer function and trainscg algorithm. The maximum neurons studied for cylinders and slices were 80 and 50 respectively, starting with a minimum of 1 neuron and then increasing the network size in steps by adding a neuron each time. Table 2 shows the effect of varying number of neurons of ANN model on food temperature prediction results. As can be seen, for cylinders, the ANN prediction is not very sensitive up to 60 neurons and beyond that the errors increase significantly. On the other hand, the errors are increasing rapidly beyond 10 neurons for slices indicating that the prediction results are highly sensitive to number of neurons. In addition, based on error analysis results, it is found that the ANN model is not very sensitive till 6 numbers of neurons for both the slice and cylindrical samples and the lowest error is found with 4 hidden neurons. Thus the ANN model with 4 neurons is selected for studying the influence of transfer functions and training algorithms on model prediction capability.

**Table 1**
List of transfer functions and back propagation training algorithms used in ANN training.

| Sl. no. | Transfer function | Training algorithms |
|---|---|---|
| 1 | logsig (Log sigmoid) | scg (Scaled conjugate gradient back propagation) |
| 2 | tansig (Hyperbolic tangent sigmoid) | cgp (Polak–Ribiere conjugate gradient back propagation) |
| 3 | poslin (Positive linear) | bfg (BFGS quasi-Newton back propagation) |
| 4 | satlin (Saturating linear) | lm (Levenberg–Marquardt back propagation) |
| 5 | – | rp (Resilient back propagation; Rprop) |

**Table 2**
Results of measures of error in food temperature prediction results of ANN model considering logsig transfer function and trainscg algorithm for different number of neurons.

| Measures of error | Number of neurons | | | | | | | |
|---|---|---|---|---|---|---|---|---|
| | Cylinder | | | | Slice | | | |
| | 4 | 50 | 60 | 80 | 4 | 10 | 20 | 50 |
| Mean absolute error (MAE) | 0.633 | 0.681 | 0.668 | 1.120 | 0.475 | 0.500 | 0.758 | 1.023 |
| Root mean square error (RMSE) | 0.769 | 0.792 | 0.944 | 1.396 | 0.670 | 0.691 | 1.436 | 1.697 |
| Standard error (SE) | 0.213 | 0.219 | 0.261 | 0.386 | 0.146 | 0.151 | 0.313 | 0.370 |
| Correlation coefficient ($R^2$) | 0.950 | 0.947 | 0.926 | 0.842 | 0.975 | 0.973 | 0.889 | 0.846 |

**Table 3**
Results of measures of error in food temperature prediction results of ANN model considering 4 neurons and trainscg algorithm for different transfer functions.

| Measures of error | Transfer functions | | | | | | | |
|---|---|---|---|---|---|---|---|---|
| | Cylinder | | | | Slice | | | |
| | logsig | tansig | satlin | poslin | logsig | tansig | satlin | poslin |
| Mean absolute error (MAE) | 0.633 | 0.642 | 0.675 | 0.967 | 0.475 | 0.524 | 0.606 | 0.632 |
| Root mean square error (RMSE) | 0.769 | 0.798 | 0.848 | 1.161 | 0.670 | 0.741 | 0.744 | 0.860 |
| Standard error (SE) | 0.213 | 0.221 | 0.235 | 0.321 | 0.146 | 0.161 | 0.162 | 0.188 |
| Correlation coefficient ($R^2$) | 0.950 | 0.947 | 0.940 | 0.889 | 0.975 | 0.970 | 0.969 | 0.960 |

For further refinement of ANN configuration, ANN model with 4 neurons and trainscg algorithm for each of potato geometry is subjected for sensitivity study of various transfer functions (Table 1) to find the most appropriate transfer function so that the resultant network can simulate the experiments with minimum measures of error. Table 3 presents the results of error analysis indicating the influence of different transfer functions on prediction capability of ANN model. As can be seen, the network with logsig transfer function performs the best in terms errors for each of sample geometry.

In order to obtain accurate and reliable network model, there is need to examine the influence of several training algorithms namely scg, cgp, bfg, lm and rp listed in Table 1 on obtained network configuration with 4 neurons and logsig transfer function and find the best training algorithm, that can make ANN model most effective in simulation of the experiments. Results of error analysis showing the influence of different training algorithms on food temperature prediction of ANN model are presented in Table 4. It is worth noting that out of various training algorithms investigated, the trainrp algorithm provides the best results for both cylinders and slices in terms of minimum errors. On the other hand, the trainlm and traincgp algorithms produce the maximum deviations in prediction results from experiments for cylinders and slices respectively.

Based on results of present investigation, it can be concluded that for both cylinders and slices, the neural network model with 4 neurons and logsig transfer function with trainrp back propagation algorithm gives the best accuracy in terms of lowest measures of error and hence it is considered the most appropriate ANN model.

### 3.2. Analytical heat diffusion model

The governing equation describing transient heat diffusion through a sample in one-dimensional Cartesian and cylindrical coordinates for infinite slice and infinite cylinder can be written in the following compact form [19]:

$$a\left(\frac{1}{z^n}\right)\left(\frac{\partial}{\partial z}\right)\left[z^n\left(\frac{\partial T_p}{dz}\right)\right]=\frac{\partial T_p}{\partial t} \tag{5}$$

where, $n=0$, $z=x$ for infinite slice and $n=1$, $z=r$ for infinite cylinder. $z$ and $t$ are the space and time coordinates respectively. Some simplifying assumptions have been made: (i) Moisture evaporation occur at the surface of the solid. (ii) Temperature and moisture content are initially uniform within the solid.

**Table 4**
Results of measures of error in food temperature prediction results of ANN model considering 4 neurons and logsig transfer function for different training algorithms.

| Measures of error | Training algorithms | | | | | | | | | |
|---|---|---|---|---|---|---|---|---|---|---|
| | Cylinder | | | | | Slice | | | | |
| | trainrp | trainscg | traincgp | trainbfg | trainlm | trainrp | trainscg | traincgp | trainbfg | trainlm |
| Mean absolute error (MAE) | 0.618 | 0.633 | 0.882 | 1.202 | 1.198 | 0.446 | 0.475 | 0.616 | 0.484 | 0.509 |
| Root mean square error (RMSE) | 0.752 | 0.769 | 1.103 | 1.632 | 1.648 | 0.599 | 0.670 | 0.809 | 0.676 | 0.708 |
| Standard error (SE) | 0.208 | 0.213 | 0.305 | 0.451 | 0.456 | 0.131 | 0.146 | 0.176 | 0.147 | 0.154 |
| Correlation coefficient ($R^2$) | 0.952 | 0.950 | 0.900 | 0.788 | 0.784 | 0.980 | 0.975 | 0.963 | 0.974 | 0.972 |

The initial and boundary conditions when a moist body is heated in a medium and moisture evaporates at the surface are given as:

$$T_p(z,0) = T_{po} \tag{6}$$

$$\frac{\partial T_p(0,t)}{\partial z} = 0 \tag{7}$$

$$-k_p \frac{\partial T_p(Z,t)}{\partial z} + h_c\big[T - T_p(Z,t)\big] - \lambda \cdot W(t) = 0 \tag{8}$$

where $Z = L$ for infinite slice (half thickness) and $Z = R$ (radius) for infinite cylinder. $\lambda$ and $W(t)$ are the latent heat of evaporation and drying rate respectively. The drying rate can be expressed as:

$$W(t) = k_o e^{-kt} \tag{9}$$

where $k_o$ and $k$ represent the lag factor and drying constant of characteristic drying curve respectively. Substituting Eq. (9) into Eq. (8), the boundary condition becomes:

$$-\frac{\partial T_p(Z,t)}{\partial z} + \frac{h_c}{k_p}\big[T - T_p(Z,t)\big] - \frac{\lambda}{k_p}\big[k_o e^{-kt}\big] = 0 \tag{10}$$

In the present analysis, Laplace transform because of its simple formulation and general acceptability, is applied to solve the heat diffusion equation for food sample temperature prediction during solar drying.

*3.2.1. Cylinder*

The solution of Eq. (5) for cylinder under boundary conditions represented by Eqs. (6) and (7) in the form of Laplace transform $T_p(r,s)$ is given as [20]:

$$T_p(r,s) - \frac{T_{po}}{s} = A I_o\left[r\left(\frac{s}{a}\right)^{1/2}\right] \tag{11a}$$

where $I_o\{r(\sqrt{s/a})\}$ is the modified Bessel function of the first kind and zeroth order.

Put $y = (s/a)$.

Eq. (11a) simplifies to

$$T_p(r,s) - \frac{T_{po}}{s} = A I_o\big[r(\sqrt{y})\big] \tag{11}$$

Transforming Eq. (10) gives:

$$-T_p'(R,s) + \frac{h_c}{k_p}\left[\frac{T}{s} - T_p(R,s)\right] - \frac{\lambda}{k_p}\left[\frac{k_o}{s+k}\right] = 0 \tag{12}$$

Combining Eqs. (11) and (12), the constant $A$ can be found as:

$$A = \frac{h_c(T - T_{po}) - \lambda(\frac{k_o}{s+k})}{sk_p[\sqrt{y}\cdot I_1\{\sqrt{y}\cdot R\} + \frac{h_c}{k_p}\cdot I_o\{\sqrt{y}\cdot R\}]} \tag{13}$$

Substituting the value of $A$ in Eq. (11), one gets:

$$T_p(r,s) - \frac{T_{po}}{s} = \frac{[h_c(T - T_{po}) - \lambda(\frac{k_o}{s+k})]I_o\{\sqrt{y}\cdot r\}}{sk_p[\sqrt{y}\cdot I_1\{\sqrt{y}\cdot R\} + \frac{h_c}{k_p}\cdot I_o\{\sqrt{y}\cdot R\}]} \tag{14}$$

The solution of Eq. (14) is obtained with the help of expansion theorem [20]:

$$\begin{aligned}\frac{T_p(r,t) - T_{po}}{T - T_{po}} &= 1 - \frac{\theta_{wb}\cdot J_o\{(Pd)^{1/2}\frac{r}{R}\}}{[J_o(Pd)^{1/2} - (1/Bi_h)(Pd)^{1/2}\cdot J_1(Pd)^{1/2}]}\exp\big[-Pd\,Fo\big] \\ &\quad - \sum_{n=1}^{\infty}\left[1 - \frac{\theta_{wb}}{1 - (Pd/\mu_n^2)}\right]A_n\cdot\cos\mu_n\frac{r}{R}\cdot\exp\big[-\mu_n^2 Fo\big]\end{aligned} \tag{15}$$

where,

$$A_n = \frac{2Bi_h}{J_o(\mu_n)[\mu_n^2 + Bi_h^2]}$$

$\mu_n$ are the roots of the characteristic equation

$$\frac{J_o(\mu)}{J_1(\mu)} = \frac{1}{Bi_h}\mu; \qquad Bi_h = \frac{h_c R}{k_p}; \qquad Fo = \frac{at}{R^2}; \qquad Pd = \frac{kR^2}{a}$$

is the Predvoditelev criterion; $a = k_p/(\rho C_p)$ is thermal diffusivity and $\theta_{wb} = \lambda k_o/h_c(T - T_{po})$ is characteristic temperature.

In the present investigation, the experimental transient food sample temperatures are obtained as the average temperatures of the sample during drying. In order to validate the prediction model, there is a need to compare the experimental and prediction results of mean food sample temperature. Thus, the mean transient sample temperature for cylinder can be obtained by integrating Eq. (15) over the whole volume. The solution is:

$$\begin{aligned}\frac{\overline{T}_p(t) - T_{po}}{T - T_{po}} &= 1 - \frac{2\theta_{wb}\cdot J_1(Pd)^{1/2}}{[(Pd)^{1/2}J_o(Pd)^{1/2} - (1/Bi_h)Pd\cdot J_1(Pd)^{1/2}]}\exp[-Pd\,Fo] \\ &\quad - \sum_{n=1}^{\infty}\left[1 - \frac{\theta_{wb}}{1 - (Pd/\mu_n^2)}\right]B_n\cdot\exp\big[-\mu_n^2 Fo\big]\end{aligned} \tag{16}$$

where $B_n$ are the constant coefficients determined by the relation:

$$B_n = \frac{2J_1(\mu_n)}{\mu_n}A_n = \frac{4Bi_h^2}{\mu_n^2(\mu_n^2 + Bi_h^2)}$$

*3.2.2. Slice*

Similarly for slice, the Laplace transform $T_p(x,s)$ for the transient heat diffusion equation (Eq. (5)) with boundary conditions (Eqs. (6) and (7)) is given as [20]:

$$T_p(x,s) - \frac{T_{po}}{s} = A\cdot\cosh\left[\left(\frac{s}{a}\right)^{1/2}\cdot x\right] \tag{17a}$$

Putting $y = (s/a)$ and Eq. (17a) simplifies to

$$T_p(x,s) - \frac{T_{po}}{s} = A\cdot\cosh\big[(\sqrt{y})\cdot x\big] \tag{17}$$

Transforming Eq. (10) gives:

$$-T_p'(L,s) + \frac{h_c}{k_p}\left[\frac{T}{s} - T_p(L,s)\right] - \frac{\lambda}{k_p}\left[\frac{k_o}{s+k}\right] = 0 \tag{18}$$

Combining Eqs. (17) and (18), the constant $A$ can be found as:

$$A = \frac{(T - T_{po})(s+k) - y\cdot\lambda\cdot k_o}{s(s+k)\big[\cosh\{\sqrt{y}\cdot L\} + \frac{h_c}{k_p}\cdot y\cdot\sinh\{\sqrt{y}\cdot L\}\big]} \tag{19}$$

Substituting the value of $A$ in Eq. (17), one gets:

$$T_p(x,s) - \frac{T_{po}}{s} = \frac{[(T - T_{po})(s+k) - y\cdot\lambda\cdot k_o]\cosh[\sqrt{y}\cdot x]}{s(s+k)\big[\cosh\{\sqrt{y}\cdot L\} + \frac{h_c}{k_p}\cdot\sqrt{y}\cdot\sinh\{\sqrt{y}\cdot L\}\big]} \tag{20}$$

The solution of Eq. (20) is obtained with the help of expansion theorem [20]:

$$\begin{aligned}\frac{T_p(x,t) - T_{po}}{T - T_{po}} &= 1 - \frac{\theta_{wb}\cdot\cos\big\{(Pd)^{1/2}\frac{x}{L}\big\}}{\cos(Pd)^{1/2} - (1/Bi_h)(Pd)^{1/2}\sin(Pd)^{1/2}}e^{-PdF_o} \\ &\quad - \sum_{n=1}^{\infty}\left[1 - \frac{\theta_{wb}}{1 - (Pd/\mu_n^2)}\right]A_n\cdot\cos\mu_n\frac{x}{L}\cdot\exp\big[-\mu_n^2 Fo\big]\end{aligned} \tag{21}$$

where

$$A_n = \frac{2\sin\mu_n}{\mu_n + \sin\mu_n\cos\mu_n} = (-1)^{n+1}\frac{2Bi_h(Bi_h^2+\mu_n^2)^{1/2}}{\mu_n(Bi_h^2+Bi_h+\mu_n^2)}$$

and $\mu_n$ are the roots of the characteristic equation, $\cot\mu = (1/Bi_h)\mu$.

The mean sample temperature of slice is obtained by integrating Eq. (21). The solution is:

$$\frac{\overline{T_p}(t)-T_{po}}{T-T_{po}} = 1 - \frac{\theta_{wb}}{(Pd)^{1/2}[\cot(Pd)^{1/2}-(1/Bi_h)(Pd)^{1/2}]}e^{-PdF_o} - \sum_{n=1}^{\infty}\left[1-\frac{\theta_{wb}}{1-(Pd/\mu_n^2)}\right]B_n\exp[-\mu_n^2 Fo] \tag{22}$$

where

$$B_n = \frac{A_n\sin\mu_n}{\mu_n} = \frac{2Bi_h^2}{\mu_n^2(Bi_h^2+Bi_h+\mu_n^2)}$$

For Fourier number, $Fo > 0.2$, the infinite series solutions of Eqs. (16) and (22) for mean food sample temperature of cylinders and slice respectively may be approximated by the first term of the series and the characteristic parameter $\mu_1$ for cylinder and slices can be obtained from the following relation [20]:

$$\mu_1^2 = (\mu_1)_\infty^2\cdot\frac{1}{1+A_1/Bi_h^p} \tag{23}$$

where $Bi_h$ represents the Biot number for heat transfer. The $(\mu_1)_\infty$ is the value of $\mu_1$ at $Bi_h=\infty$. The values of the constants $(\mu_1)_\infty$, $A_1$ and $p$ are: for slice: $(\mu_1)_\infty = 1.5708$; $A_1 = 2.24$; $p = 1.02$ and for cylinder: $(\mu_1)_\infty = 2.4048$; $A_1 = 2.45$; $p = 1.04$.

### 3.3. Statistical model

In the present study, the classical statistical model is also studied for the prediction of food temperature variation during drying process. The input data on the experimental parameters namely solar radiation intensity, ambient air temperature during drying of cylinders and slices are individually regressed through second and third order to compute food sample temperature. The proposed regression equations are:

Second order regression

$$T_p = A_1\cdot q_s + A_2\cdot T_a + A_3\cdot q_s\cdot T_a + A_4\cdot q_s^2 + A_5\cdot T_a^2 \tag{24}$$

Third order regression

$$T_p = A_1\cdot q_s + A_2\cdot T_a + A_3\cdot q_s\cdot T_a + A_4\cdot q_s^2 + A_5\cdot T_a^2 + A_6\cdot q_s\cdot T_a^2 + A_7\cdot q_s^2\cdot T_a + A_8\cdot q_s^3 + A_9\cdot T_a^3 \tag{25}$$

where $A_1$ to $A_9$ are regression coefficients determined by Matlab programming. The performance of the proposed statistical model is evaluated for food temperature prediction by computing the various statistical measures of error represented by Eqs. (1)–(4).

## 4. Results and discussion

The experimental observations of moisture evaporated and temperature rise of food samples were recorded at regular time intervals during drying of cylindrical and slice shaped potato samples. The experimental mean food sample temperature was obtained as the average of the temperatures recorded at several locations of the sample. The first term of each infinite series solution of Eqs. (16) and (22) for heat diffusion equation was used for prediction of mean transient temperatures of potato cylinders and slices respectively. However, it requires the knowledge of numerical values of various parameters involved in their estimation. The convective heat transfer coefficient at food-air interface, $h_c$; lag factor, $k_o$ and drying constant, $k$ of characteristic drying curve of each sample geometry were determined by experiments. The experimental arrangement and methodology for determination of these coefficients are described elsewhere [21]. Accordingly, the mean values of convective heat transfer coefficients at air–food interface for cylindrical and slice geometries, based on the method of energy balance during solar drying are determined and found to be 29.85 and 22.09 $W/m^2\,°C$ respectively. In addition, the values of drying parameters $k_o$ and $k$ of characteristic drying curves of cylinders and slices are obtained by the method of non-linear regression analysis of experimental data of food moisture contents and drying time. The obtained values are; for cylinders: $k_o = 0.00024$ and $k = 0.00011$ (1/s); for slices: $k_o = 0.00021$ and $k = 0.00004$ (1/s). Furthermore, the values of specific heat capacity ($C_p$), latent heat of vaporization ($\lambda$), and density ($\rho$) of potato are taken from the empirical relations (Appendix A). The values of thermal conductivity ($k_p$) and thermal diffusivity ($a$) of the potato are also taken from published literature [22].

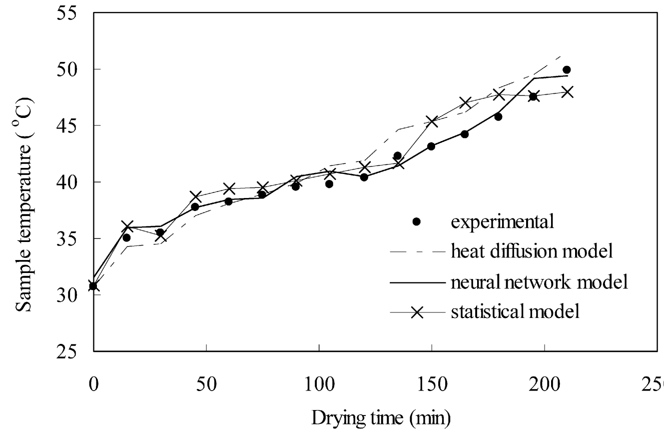


**Fig. 2.** Comparison between experimental and predicted transient food temperatures obtained from heat diffusion, neural network and statistical models for potato cylinder.

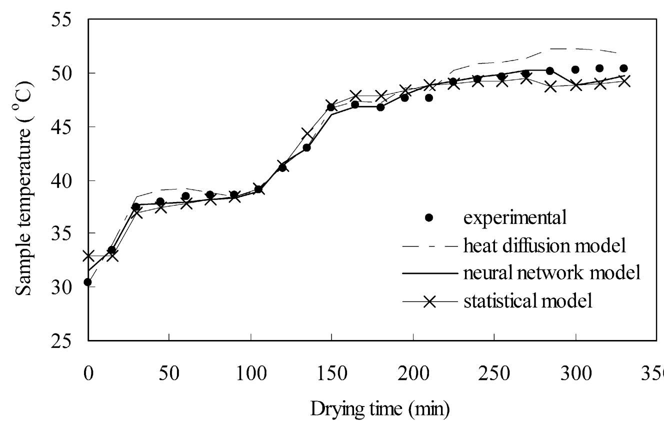


**Fig. 3.** Comparison between experimental and predicted transient food temperatures obtained from heat diffusion, neural network and statistical models for potato slice.

### 4.1. Comparison of prediction models

The accuracy of various proposed prediction models is tested through the comparison of predicted and experimental food sample temperature variation with drying time during solar drying process. Figs. 2 and 3 show the results of analysis for potato

**Table 5**
Results of error analysis for ANN, statistical and heat diffusion models.

| Measures of error | Cylinder | | | Slice | | |
|---|---|---|---|---|---|---|
| | Neural network model | Statistical model | Heat diffusion model | Neural network model | Statistical model | Heat diffusion model |
| MAE | 0.618 | 1.122 | 1.288 | 0.446 | 0.764 | 0.854 |
| RMSE | 0.752 | 1.378 | 1.549 | 0.598 | 0.961 | 1.078 |
| SE | 0.208 | 0.381 | 0.429 | 0.130 | 0.210 | 0.235 |
| $R^2$ | 0.952 | 0.846 | 0.808 | 0.980 | 0.949 | 0.936 |

cylinders and slices respectively. As can be seen, all the investigated prediction models simulate the experiments satisfactorily for both food sample geometries. However, the results predicted by ANN are found to be slightly closer to experimental data, irrespective of sample geometry. In order to appreciate these results quantitatively, the prediction capability of proposed models is further assessed on the basis of various statistical measures of error. The results of analysis are presented in Table 5. As can be observed from the table, the prediction performance of ANN model is the best, followed by statistical and heat diffusion models, thus demonstrating its worthiness for food temperature prediction during solar drying.

### 4.2. Sensitive analysis in ANN prediction

The effect of uncertainty in the values of input parameters namely solar radiation intensity and ambient air temperature on root mean square error (RMSE) in ANN prediction results has also been studied by introducing small random errors within a range of ±5% in the values of input parameters. Figs. 4(a) and 4(b) represent the results of sensitivity analysis for cylinder and slice respectively. As can be seen, the ANN prediction results have strong dependence on these parameters. However, the ANN model is slightly more sensitive to ambient air temperature compared to solar radiation intensity for both food sample geometries.

## 5. Conclusion

In the present study, the suitability of neural network model considering several possible configurations has been assessed for temperature prediction of potato cylinder and slice during solar drying. Based on error analysis results, it is concluded that the neural network with 4 neurons and logsig transfer function with trainrp back propagation algorithm is the most appropriate ANN configuration in terms of prediction capability of transient food temperature for both food geometries. The results of comparative

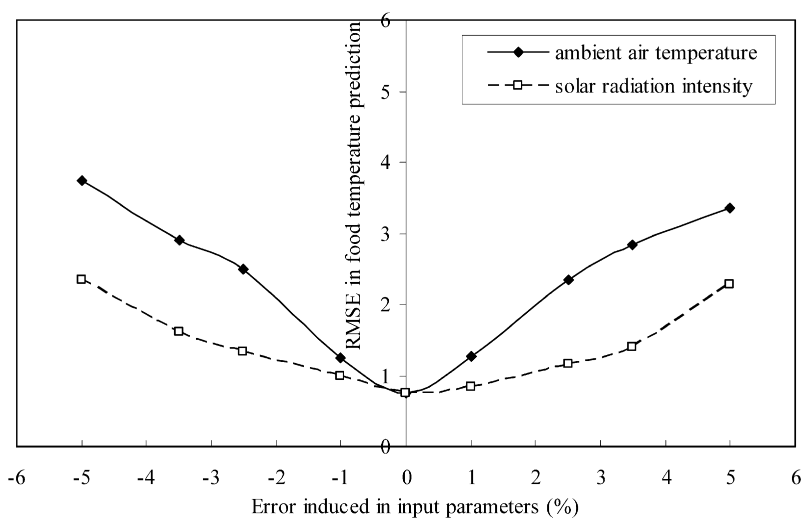


(a)

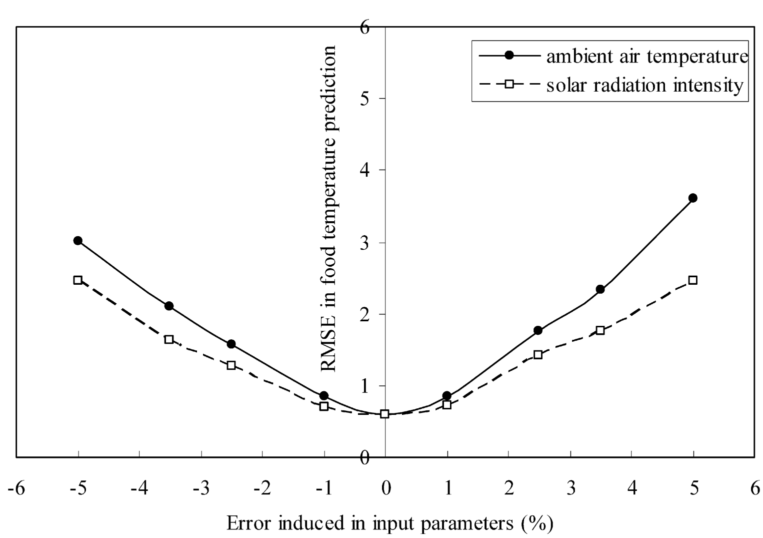


(b)

**Fig. 4.** (a) Effect of induced error in input parameters on root mean square error (RMSE) in food temperature prediction for potato cylinder. (b) Effect of induced error in input parameters on root mean square error (RMSE) in food temperature prediction for potato slice.

study on prediction capability of optimal ANN with heat diffusion and statistical models reveal that the ANN model can simulate the experiments the best, followed by statistical and diffusion models, thus justifying its suitability in solar drying application.

The ANN model proposed in the present study is simple to understand and can easily implemented with the help of simple Matlab program by readers. It is believed that this study would prove to be an effective tool among researchers, food process engineers, designers of solar dryer for on-line state estimation and optimal control of solar drying process without requiring exhaustive experimentation, thus saving both time and money.

## Acknowledgements

The authors gratefully acknowledge Ministry of New and Renewable Energy (Government of India), New Delhi for providing financial assistance to the first author for carrying out the present work.

## Appendix A. Thermo-physical parameters estimation

The following expressions were used for calculating thermo-physical properties for potato in the present work:

1. Latent heat of vaporization, $\lambda$ [23]:

$$\lambda = 4186.8\{597 - 0.56(T + 273)\} \tag{A.1}$$

2. Specific heat, $C_p$ [24]:

$$C_p = 4.184 \times 10^3(0.406 + 0.00146T + 0.203M - 0.0249M^2) \tag{A.2}$$

3. Density of potato, $\rho$ [25]:

$$\rho = \left(A + B\exp(CM^2)\right) \times 1000 \tag{A.3}$$

where $A$, $B$ and $C$ are correlation coefficients.

## References

[1] A. Arata, V.K. Sharma, G. Spagna, Performance evaluation of solar assisted dryers for low temperature drying application. II. Experimental results, Energy Conversion and Management 34 (1993) 417–426.
[2] J. Saguy, S. Mizrahi, R. Villota, M. Karel, Accelerated method for determining the kinetic model of ascorbic acid loss during dehydration, Journal of Food Science 43 (1978) 1861.
[3] B. Hallstrom, C. Skjoldebrand, C. Tragardt, Heat Transfer and Food Products, Elsevier Applied Sci., New York, 1988.
[4] R.P. Singh, Heating and cooling processes for foods, in: D.R. Heldman, D.B. Lund (Eds.), Handbook of Food Engineering, Marcel Dekker Inc., New York, 1992.
[5] R.K. Goyal, G.N. Tiwari, Performance of a reverse flat plate absorber cabinet dryer: a new concept, Energy Conversion and Management 40 (4) (1999) 385–392.
[6] D. Jain, G.N. Tiwari, Effect of greenhouse on crop drying under natural and forced convection II. Theoretical modeling and experimental validation, Energy Conversion and Management 45 (2004) 2777–2793.
[7] G.N. Tiwari, P.S. Bhatia, A.K. Singh, R.F. Sutar, Design parameters of a shallow bed solar crop dryer with reflector, Energy Conversion and Management 35 (6) (1994) 535–542.
[8] N. Rahman, S. Kumar, Transient temperature analysis of potato during drying: theoretical modeling and experimental validation, International Journal of Ambient Energy 27 (4) (2006) 171–180.
[9] S.A. Kalogirou, Applications of artificial neural-networks for energy systems, Applied Energy 67 (1–2) (2000) 17–35.
[10] S.A. Kalogirou, Artificial neural networks in renewable energy systems applications: a review, Renewable and Sustainable Energy Reviews 5 (2001) 373–401.
[11] H. Kurt, K. Atik, M. Özkaymak, Z. Recebli, Thermal performance parameters estimation of hot box type solar cooker by using artificial neural network, International Journal of Thermal Sciences 47 (2) (2008) 192–200.
[12] S.A. Kalogirou, S. Panteliou, A. Dentsoras, Artificial neural networks used for the performance prediction of a thermo-siphon solar water heater, Renewable Energy 18 (1–2) (1999) 87–99.
[13] C. Cetiner, F. Halici, H. Cacur, I. Taymaz, Generating hot water by solar energy and application of neural network, Applied Thermal Engineering 25 (8–9) (2005) 1337–1348.
[14] B.K. Bala, M.A. Ashraf, M.A. Uddin, S. Janjai, Experimental and neural network prediction of the performance of a solar tunnel drier for drying jackfruit bulbs and leather, Journal of Food Process Engineering 28 (6) (2005) 552–566.
[15] I. Farkas, P. Geczy-Vig, Neural network modeling of flat-plate solar collectors, Computers and Electronics in Agriculture 40 (1–3) (2003) 87–102.
[16] AOAC, Official methods of Analysis, 17th ed., Association of Official Analytical Chemists, Arlington, VA, 2002.
[17] C.M. Bishop, Neural networks and their applications, Reviews on Scientific Instrumentation 65 (6) (1994) 1803–1832.
[18] K. Hornik, M. Stinchcombe, H. White, Multilayer feed forward networks are universal approximations, Neural Network 2 (1989) 359–366.
[19] I. Dincer, S. Dost, A modeling study for moisture diffusivities and moisture transfer coefficients in drying of solid objects, International Journal of Energy Research 20 (1996) 531–539.
[20] A.V. Luikov, Analytical Heat Diffusion Theory, Academic Press, New York, 1968.
[21] P.P. Tripathy, S. Kumar, Modeling of heat transfer and energy analysis of potato slices and cylinders during solar drying, Applied Thermal Engineering, in press, doi:10.1016/j.applthermaleng.2008.04.018 (Corrected proof, available online 1 May 2008).
[22] Y.A. Cengel, Heat transfer: A Practical Approach, McGraw-Hill, New York, 1998.
[23] S. Youcef-Ali, N. Moummi, J.Y. Desmons, A. Abene, H. Messaoudi, M. Le Ray, Numerical and experimental study of dryer in forced convection, International Journal of Energy Research 25 (6) (2001) 537–553.
[24] N. Wang, J.G. Brennan, The influence of moisture content and temperature on the specific heat of potato measured by differential scanning calorimetry, Journal of Food Engineering 19 (3) (1993) 303–310.
[25] N. Wang, J.G. Brennan, Changes in structure, density and porosity of potato during dehydration, Journal of Food Engineering 24 (1) (1995) 61–76.